IOP Publishing Journal of Geophysics and Engineering
J. Geophys. Eng. 14 (2017) 1349–1357 (9pp) https://doi.org/10.1088/1742-2140/aa84f5

# Extending the inverse scattering series free-surface-multiple-elimination algorithm by accommodating the source property on data with interfering or proximal seismic events

**Lei Zhao[1], Jinlong Yang[2,3,4] and Arthur B Weglein[3]**

[1] School of Ocean and Earth Science, Tongji University, Shanghai 200092, People's Republic of China
[2] SINOPEC Geophysical Research Institute, Nanjing 210014, People's Republic of China
[3] M-OSRP, University of Houston, Houston TX 77004, United States of America

E-mail: yangjl.swty@sinopec.com

Received 26 December 2016, revised 28 June 2017
Accepted for publication 8 August 2017
Published 27 September 2017

**Abstract**

The inverse scattering series free-surface-multiple-elimination (FSME) algorithm is modified and extended to accommodate the source property–source radiation pattern. That accommodation can provide additional value for the fidelity of the free-surface multiple predictions. The new extended FSME algorithm retains all the merits of the original algorithm, i.e., fully data-driven and with a requirement of no subsurface information. It is tested on a one-dimensional acoustic model with proximal and interfering seismic events, such as interfering primaries and multiples. The results indicate the new extended FSME algorithm can predict more accurate free-surface multiples than methods without the accommodation of the source property if the source has a radiation pattern. This increased effectiveness in prediction contributes to removing free-surface multiples without damaging primaries. It is important in such cases to increase predictive effectiveness because other prediction methods, such as the surface-related-multiple-elimination algorithm, has difficulties and problems in prediction accuracy, and those issues affect efforts to remove multiples through adaptive subtraction. Therefore accommodation of the source property can not only improve the effectiveness of the FSME algorithm, but also extend the method beyond the current algorithm (e.g. improving the internal multiple attenuation algorithm).

Keywords: ISS, FSME, source radiation pattern, interfering seismic events

(Some figures may appear in colour only in the online journal)

## 1. Introduction

In seismic exploration, multiple removal is a classic and long-standing problem. To remove free-surface multiples, plenty of methods have been proposed and developed with different assumptions, advantages, and limitations (e.g. Carvalho 1992, Verschuur *et al* 1990, Weglein *et al* 1997, 2003, Berkhout and Verschuur 1999, Dragoset *et al* 2008). Among these methods, the inverse scattering series (ISS) free-surface-multiple-elimination (FSME) algorithm (Carvalho 1992, Weglein *et al* 1997, 2003) is fully data-driven and requires no subsurface information, which has a big advantage, especially under conditions of complex geology. In principle, the ISS FSME algorithm is able to predict exact amplitude and time of free-surface multiples at all offsets so as to remove the free-surface multiples through a direct subtraction, and preserve primaries (Carvalho 1992, Weglein *et al* 1997). However, in practice the algorithm may require an adaptive assist.

[4] Author to whom any correspondence should be addressed.

 

In contrast, the surface-related-multiple-elimination algorithm cannot provide accurate predictions because it ignores the obliquity factor and retains the source ghosts. Hence, it requires an adaptive step in principle in practice. Certain criteria adaptive subtraction based such as energy minimization can be a reasonable choice, however in other situations, it has issues with proximal and interfering problems, because the energy minimization criterion assumes that the energy of the data will be minimized after the multiples are removed. But in some cases, after multiple removal, the energy may increase rather than decrease. Therefore, adaptive subtraction can fail to remove the multiples or can damage primaries.

The ISS method has certain prerequisites including (Weglein *et al* 2003): (1) the reference wave[5] removal, (2) the source wavelet and radiation pattern estimation and removal, and (3) the source and receiver ghosts[6] removal. Hence, preprocessing of the seismic data is the important component for free-surface multiple prediction. The reference wave should be removed because it contains no subsurface information which is the objective of the research. To separate the reference wavefield from the scattered wavefield (reflection data), Weglein and Secrest (1990) propose a method that require no subsurface information. To identify subsurface properties from seismic data, it is also necessary to identify and remove the seismic source's effect from the seismic data because both the source and the properties of the Earth contribute to the recorded seismic data (e.g. Weglein and Secrest 1990, Amundsen 1993, Osen *et al* 1998). Source and receiver de-ghosting will remove the ghost notches and enhance the low-frequency content of the seismic data (e.g. Zhang and Weglein 2005, 2006, Mayhan *et al* 2011, 2012, Mayhan and Weglein 2013). Yang (2014) discusses the impact of the source wavelet and ghosts on free-surface multiple prediction and removal. All of these preprocessing steps can be achieved based on Green's theorem wave separation methods without requiring any subsurface information. Green's theorem methods were explored by Zhang (Weglein *et al* 2002, Zhang and Weglein 2005, 2006, Zhang 2007) and developed by Mayhan (Mayhan *et al* 2011, 2012, Mayhan and Weglein 2013). Wu and Weglein (2014) extended the Green's theorem methods for the reference wave and scattered wave separation from off-shore acoustic plays to on-shore elastic plays. Green's theorem methods and the ISS FSME algorithm are consistent with each other, i.e., multidimensional and fully data-driven without any subsurface information.

In terms of data generated by a general source with a radiation pattern, the ISS FSME algorithm needs to be modified and extended because it assumes an isotropic point source, where the source has no variation of amplitude or phase with take-off angle[7]. In towed marine acquisition, a general source (e.g. air-gun array) with a radiation pattern is commonly used. Such a general source exhibits directivity in the take-off angle (Loveridge *et al* 1984); that directivity is an issue for multiple removal and attenuation and AVO analysis. Thus, in seismic processing, it is essential to characterize the source's effect on any seismic processing methods. Therefore, to accommodate a general source with a radiation pattern, the proposed method modifies and extends the ISS FSME algorithm to improve its accuracy and effectiveness in predicting multiples. The accommodation of the source radiation pattern is able to enhance the free-surface multiple predictions at all offsets if the source has a radiation pattern.

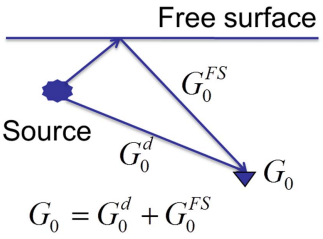


**Figure 1.** Green's function $G_0$ in the reference medium includes two parts: $G_0 = G_0^{\mathrm{d}} + G_0^{\mathrm{FS}}$. $G_0^{\mathrm{d}}$ is the direct Green's function and $G_0^{\mathrm{FS}}$ is its ghost due to the presence of free surface.

## 2. Theory

The ISS FSME subseries can be isolated and derived from the ISS (Weglein *et al* 2003, Yang 2014) as

$$D_1' = G_0^{\mathrm{d}} V_1 P_0^{\mathrm{d}}, \tag{1}$$

$$D_2' = G_0^{\mathrm{d}} V_2' P_0^{\mathrm{d}} = -G_0^{\mathrm{d}} V_1 G_0^{\mathrm{FS}} V_1 P_0^{\mathrm{d}}, \tag{2}$$

$$\vdots$$

$$D_n' = G_0^{\mathrm{d}} V_n' P_0^{\mathrm{d}} = -G_0^{\mathrm{d}} V_1 G_0^{\mathrm{FS}} V_{n-1}' P_0^{\mathrm{d}}, \tag{3}$$

where $D_1'$ is the source–receiver deghosted data. $G_0^{\mathrm{d}}$ and $G_0^{\mathrm{FS}}$ are the two parts of Green's function $G_0$—the direct arrival part and its free-surface reflection part, as shown in figure 1. $G_0^{\mathrm{d}}$ is an impulse response, and $P_0^{\mathrm{d}}$ is the direct wave generated by a general source. $V$ is the scattering factor, which is the difference between the actual and reference media. $V$ can be described as a series $V = V_1 + V_2 + \cdots + V_n$, $V_n$ is the part of $V$. $V_n'$ is the portion of $V_n$ due to the presence of the free surface. $D_n'$ (for $n > 1$) is the corresponding free-surface multiple.

For an isotropic point source, the ISS FSME algorithm (equation (3)) in a 2D case (Carvalho 1992) can be written

[5] The wave that travels in the reference medium is called a reference wave, which includes the direct wave and its ghost. The direct wave travels straightly from the source to the receiver. The ghost propagates up to the free surface and reflects down to the receiver.

[6] Ghosts are the events that by travel up to the free-surface (source ghosts) at the beginning or travel down from the free-surface to the receiver (receiver ghosts) at the end. The event that exhibits both features is called a source-receiver ghost.

[7] Take-off angle refers to the angle of incidence wave.

explicitly as

$$D_n'(k_g, k_s, \omega) = \frac{1}{\mathrm{i}\pi A(\omega)} \times \int \mathrm{d}k D_1'(k_g, k, \omega) q \mathrm{e}^{\mathrm{i}q(\epsilon_g+\epsilon_s)} D_{n-1}'(k, k_s, \omega), \quad (4)$$

where $k_g$, $k_s$ represent the receiver and the source horizontal wavenumber respectively. $\omega$ is the frequency. $\epsilon_g$ and $\epsilon_s$ are the receivers' and sources' depth below the free surface, respectively. The term $q$ is the obliquity factor $q = \mathrm{sgn}(\omega)\sqrt{\omega^2/c_0^2 - k^2}$. $c_0$ is the reference velocity. $A(\omega)$ is the source signature, which is a function of time or $\omega$ in different domains. The free-surface multiples are predicted order-by-order and then added together to give the data

$$D'(k_g, k_s, \omega) = \sum_{n=1}^{\infty} D_n'(k_g, k_s, \omega), \quad (5)$$

that have been deghosted and free-surface demultipled.

The ISS FSME algorithm (equation (4)) assumes an isotropic point source. Hence, if all the prerequisites are satisfied, Zhang (2007) has shown that this algorithm (equation (4)) has the ability to predict correct free-surface multiples at all offsets for data generated by an isotropic point source and remove these multiples from the data without adaptive subtraction. However, in terms of data generated by a general source with a radiation pattern, however, the algorithm (equation (4)) predicts free-surface multiples only approximately. To accommodate the sources' effect, the ISS FSME algorithm is modified and extended from an isotropic point source to a general source $\rho$ with a radiation pattern

$$D_n'(k_g, k_s, \omega) = \frac{1}{\mathrm{i}\pi} \int \frac{\mathrm{d}k}{\rho(k, q, \omega)} \times D_1'(k_g, k, \omega) q \mathrm{e}^{\mathrm{i}q(\epsilon_g+\epsilon_s)} D_{n-1}'(k, k_s, \omega), \quad (6)$$

where $\rho(k, q, \omega)$ is the projection of the source signature that projects the source onto the measurement surface in the $f$–$k$ domain and $k^2 + q^2 = \omega^2/c_0^2$. The details of the derivation of equation (6) can be found in appendix A. The projection of the source signature $\rho(k, q, \omega)$ can be achieved from the direct reference wavefield, which is separated from the total wavefield by using Green's theorem methods (Weglein and Secrest 1990, Mayhan and Weglein 2013, Tang *et al* 2013).

In this paper, the source array is assumed to be invariant from one shot to the next. In other words, the geometry or the distribution of the source array keeps consistency for each shot. The direct reference wavefield $P_0^{\mathrm{d}}$ for a 2D case can be expressed as an integral of the direct reference Green's function $G_0^{\mathrm{d}}$ over all air-guns in an array,

$$P_0^{\mathrm{d}}(x, z, x_s, z_s, \omega) = \iint \mathrm{d}x' \mathrm{d}z' \rho(x', z', \omega) \times G_0^{\mathrm{d}}(x, z, x' + x_s, z' + z_s, \omega), \quad (7)$$

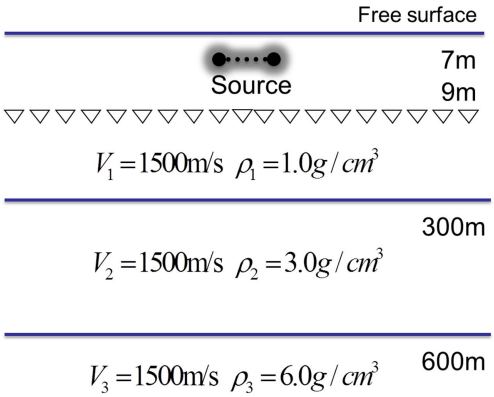


**Figure 2.** One-dimensional two-reflector acoustic model with constant velocity and varying density. Two reflectors are at 300 and 600 m. The depths of the sources and receivers are 7 m and 9 m, respectively.

where $(x, z)$ and $(x_s, z_s)$ are the prediction point and the source point, respectively. Here, $(x', z')$ is the distribution of the source with respect to the source locator $(x_s, z_s)$. Using the bilinear form of Green's function and Fourier transforming over $x$, the proposed method obtain the relationship between $\rho$ and $P_0^{\mathrm{d}}$ in the $f$–$k$ domain as

$$P_0^{\mathrm{d}}(k, z, x_s, z_s, \omega) = \rho(k, q, \omega) \frac{\mathrm{e}^{\mathrm{i}q|z-z_s|}}{2\mathrm{i}q} \mathrm{e}^{-\mathrm{i}kx_s}, \quad (8)$$

where $\rho(k, q, \omega)$ can be derived from the direct reference wavefield and $k^2 + q^2 = \omega^2/c_0^2$. The derivation of equation (8) can be found in appendix B. The parameter $q$ is not a free variable, hence we can not obtain $\rho(x, z, \omega)$ in the space-frequency domain by taking an inverse Fourier transform on $\rho(k, q, \omega)$. However, the projection of the source signature $\rho(k, q, \omega)$ can always be achieved directly from the reference wavefield $P_0^{\mathrm{d}}$ in the $f$–$k$ domain, where the variable $k$ or $q$ represents the amplitude variations of the source signature with angles. Ikelle *et al* (1997) also proposed a similar quantity, $A(k, \omega)$, the inverse source wavelet, and solved for it indirectly using the energy minimization criterion. We instead apply Green's theorem wave separation methods to get the generalized source signature directly.

By substituting the projection of the source signature $\rho(k, q, \omega)$ into the ISS FSME subseries (equations (1)–(3)), we can obtain the new extended FSME algorithm which accommodates a general source with a radiation pattern and can provide additional value by improving the fidelity of the free-surface multiple predictions at all offsets. The new extended FSME algorithm is consistent with Green's theorem wave separation methods that provides all data requirements as well as they are both fully multidimensional and require no subsurface information. The new extended FSME algorithm (equation (6)) can be reduced to the previous FSME algorithm (equation (4)) when the general source (e.g. source array) reduces to an isotropic point source. Meanwhile the projection of the source signature $\rho(k, q, \omega)$ can be applied into

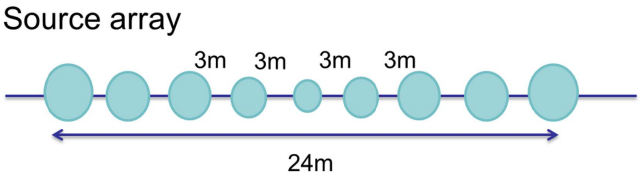


**Figure 3.** Source array with nine air-guns.

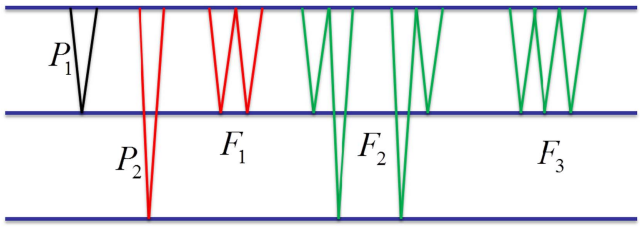


**Figure 4.** Seismic events. $P_1$ and $P_2$ are the two primaries. $F_1$, $F_2$ and $F_3$ are the first first-order, second first-order, and first second-order free-surface multiples, respectively. The events with the same color have the same arrival time.

the ISS internal multiple attention algorithm (Yang and Weglein 2015) to improve its effectiveness and accuracy, and the extension of the ISS demultiple algorithms can be easily extended to the 3D case.

## 3. Numerical tests

This section will show the impact of free-surface multiple removal through the use of the ISS FSME algorithms that are accommodating compared to not accommodating the source radiation pattern. The numerical test is based on a 1D two-reflector acoustic model with constant velocity and varying density, as shown in figure 2. Here, the constant velocity model is selected because the interfering events can completely cancel each other in this model, otherwise, they can only cancel part of events. To generate this data with interfering events, the analytic method is used in the $k$–$\omega$ domain and generate them separately. The parameters are designed so that the second primary can cancel the first-order free-surface multiple. Even though the sources and receivers are not on the free surface, the second primary and the first-order free-surface multiple have the same travel time, because both events have the same time-shift due to the depth of the source and receiver. The data are generated by a general source (e.g. source array) with a radiation pattern (figure 3) using the reflectivity method. Here it is referred to as the source-array data. The source array has nine air-guns with each a different amplitude indicated by their size. The model has two reflectors, at 300 and 600 m. The depths of the sources and receivers are at 7 m and 9 m, respectively. Here the data is assumed to have been pre-processed by removing its reference wavefield and ghosts to satisfy the prerequisites of the ISS FSME algorithm.

Primaries and free-surface multiples are generated separately as shown in figure 4. $P_1$ and $P_2$ are the two primaries. $F_1$, $F_2$ and $F_3$ are the first first-order, second first-order, and first second-order free-surface multiples, respectively. The events in the same color has the same arrival time, hence, they are interfering in the seismic data. $P_2$ and $F_1$ have opposite polarity but the same amplitude. Therefore, $P_2$ and $F_1$ cancel each other and are invisible in the seismic data. Similarly, $F_3$ will be interfere with $F_2$ and cancel part of $F_2$. Figure 5(a) represents the two primaries $P_1$ and $P_2$, and figure 5(b) is the free-surface multiples $F_1$, $F_2$ and $F_3$. Adding up them to get the total source-array data, as shown in figure 5(c). The second primary is destructively interfering with the first-order free-surface multiple and they are invisible in the seismic data. Therefore, the adaptive subtraction method can be invalid or fail for this kind of situation, because it is based on the energy minimization criterion with the assumption that the energy of the data will be minimized after the multiples are removed. However, in this case, the energy increases after removal of the first-order free-surface multiple.

The free-surface multiples will be predicted and removed from the source-array data (figure 5(c)) by using the ISS FSME algorithm (equation (4)) that does not accommodate the source radiation pattern and the new extended algorithm (equation (6)) that does accommodate the source radiation pattern. Since the synthetic data has only two orders of the free-surface multiples, the FSME algorithm needs only calculate with the second iterations. Figures 6(a) and (b) show the free-surface multiples predicted by use of the algorithms that are not accommodating and accommodating the source radiation pattern (equations (4) and (6)), respectively. Figure 6(c) is the corresponding difference between these two predictions. This is an advantage of the ISS FSME algorithm, because we need only calculate the FSME algorithm to the order that has in the actual data. The total data (figure 5(c)) will input into the ISS FSME algorithm, and figures 7(a) and (b) are the results following free-surface multiple removal by using the these two algorithms, respectively. It can be seen that both algorithms can effectively remove the free-surface multiples and recover the second primary. Figure 7(a) indicates that if the algorithm does not accommodate the source radiation pattern, the free-surface multiple removal result obtains some residues for the source-array data. The new extended algorithm that accommodates the source radiation pattern can accurately predict and completely eliminate the free-surface multiples as shown in figure 7(b).

The proposed method picks one trace (for instance, at 1800 m offset) from figures 7(a) and (b) and compare them with the trace picked from figure 5(a) to judge whether the second primary is fully recovered or not. Figure 8 illustrates the details of this single trace comparison. After removal of free-surface multiples by using the new extended algorithm, the second primary (dashed green line) is fully recovered as the original primary (red line) and second-order free-surface multiples are also completely removed. Without the algorithm accommodating the source radiation pattern, the

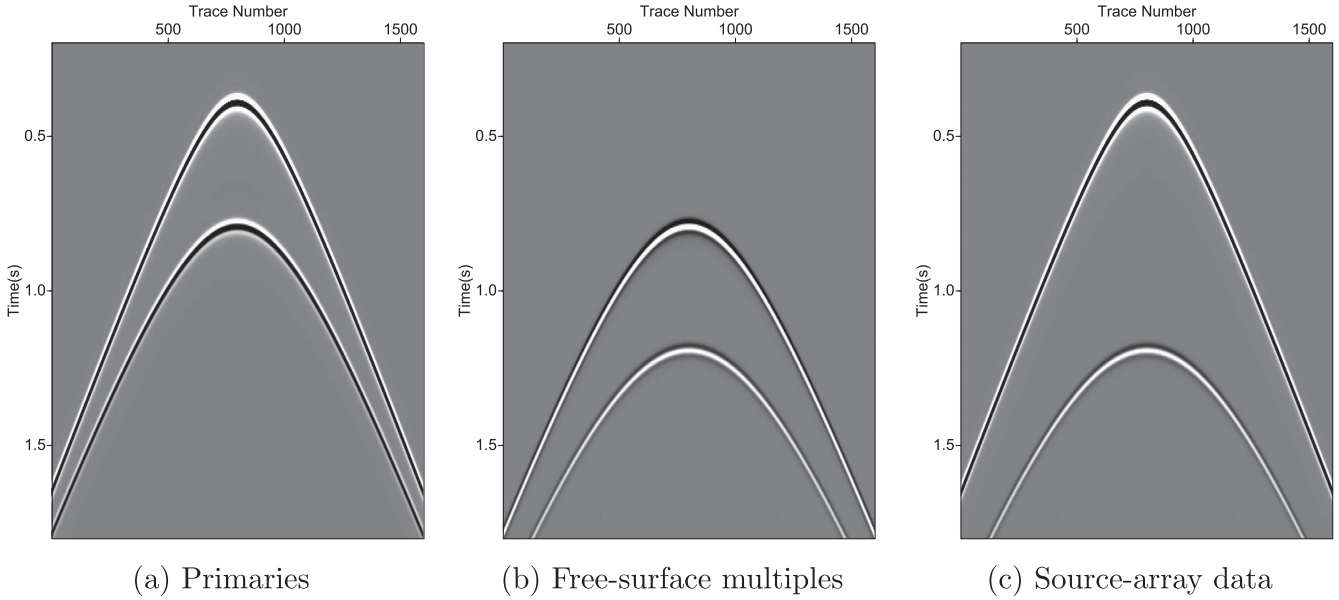


**Figure 5.** Separated seismic data: (a) primaries, (b) free-surface multiples, and (c) total source-array data.

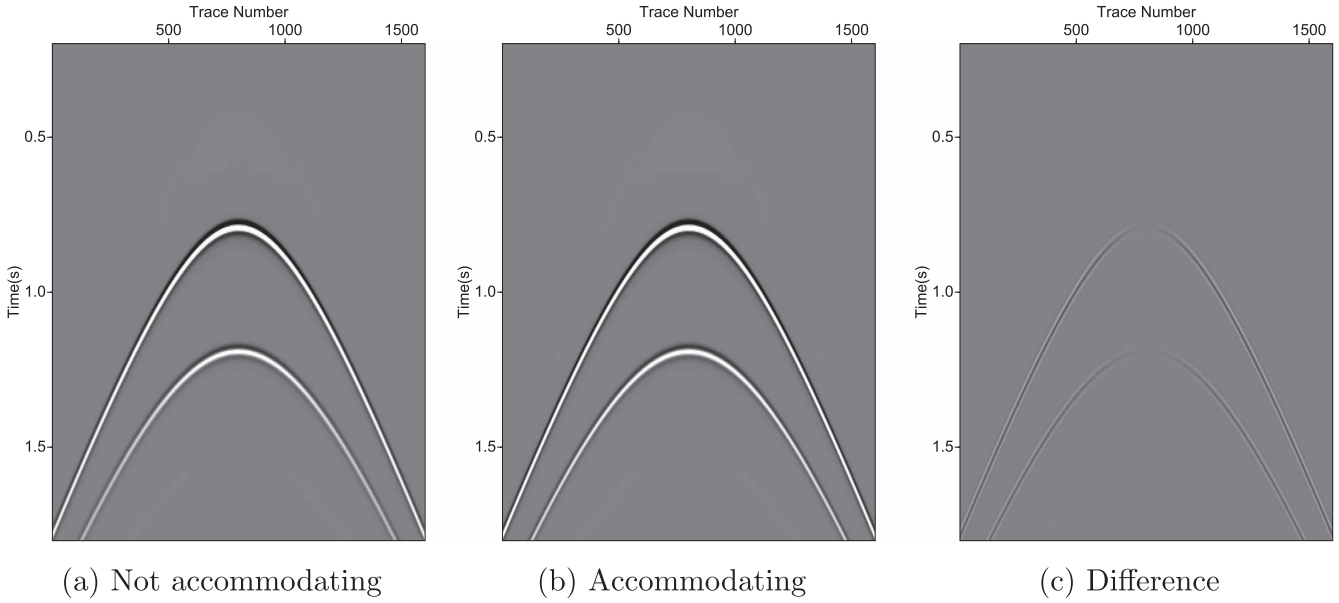


**Figure 6.** The free-surface multiples that are predicted by the ISS FSME algorithms that are (a) not accommodating and (b) accommodating the source radiation pattern. (c) The difference between these two predictions.

second primary (blue line) is partly recovered and is a little weaker than the original primary (red line) and there are some multiple residues on the second-order free-surface multiples. The amplitude errors will greatly affect AVO analysis. The numerical tests for the synthetic data with interfering events have demonstrated that the ability of the new extended ISS FSME algorithm to correctly predict both amplitude and time of free-surface multiples, as well as remove them completely without touching the primaries. Most importantly, this new extended algorithm recovers the primary that is destructively interfering with a free-surface multiple. In summary, by accommodating the source radiation pattern, the effectiveness and accuracy of the ISS FSME algorithm has been enhanced.

## 4. Conclusions

The ISS FSME algorithm is modified and extended by accommodating the source radiation pattern. Compared with previous methods the new extended algorithm can provide additional value by improving the fidelity of amplitude and phase predictions of free-surface multiples at all offsets. It is multidimensional without the requirement of any subsurface

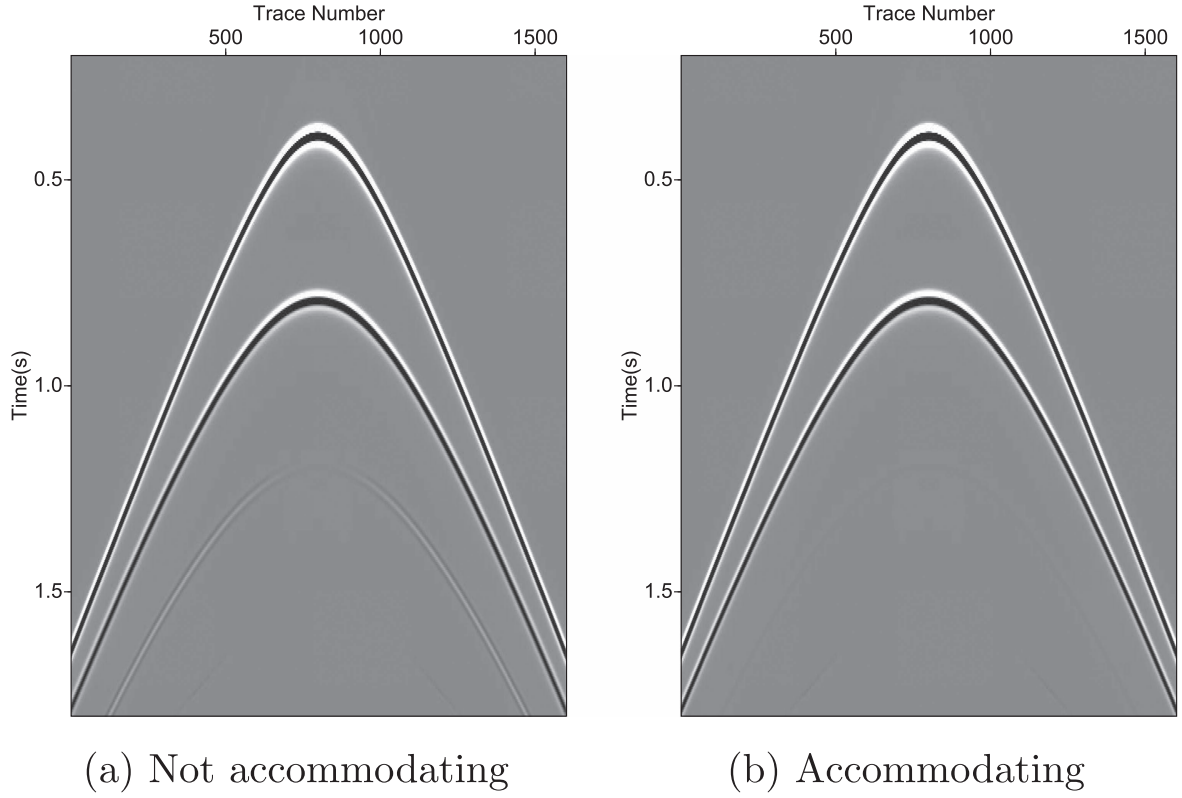


**Figure 7.** The impact of the source radiation pattern on free-surface multiple removal by using the ISS FSME algorithms that are (a) not accommodating and (b) accommodating the source radiation pattern.

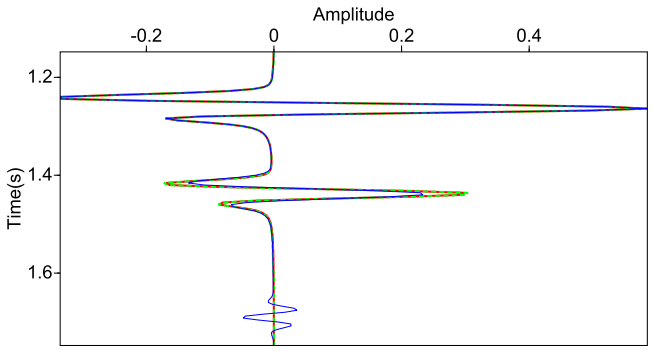


**Figure 8.** Single trace comparison: red line: the two original primaries; blue line: the result after multiple removal by using the algorithm that does not accommodate the source radiation pattern; dashed green line: the result after multiple removal using the algorithm that accommodate the source radiation pattern.

information. The numerical tests show that the new extended FSME algorithm can predict the free-surface multiples more accurately and then remove them more effectively. This accommodation and extension is particularly important when the free-surface multiples are proximal to or interfering with other events, since we cannot fix the errors in amplitude and phase of the prediction adaptively. In conclusion, the accommodation of the source radiation pattern into the FSME algorithm can not only improve the effectiveness of the algorithm, but also extend the method beyond the current algorithm (e.g. improving internal multiple attenuation algorithm).

## Acknowledgments

We are grateful to the M-OSRP sponsors for their encouragement and support. We also would like to thank SINOPEC management for permission to publish this paper.

## Appendix A. Derivation of equation (6)

Before deriving equation (6), we first derive equation (1) in a 2D case,

$$D_1'(x_g,\,\epsilon_g,\,x_s,\,\epsilon_s,\,\omega) = \int^{(4)} G_0^{\mathrm{d}}(x_g,\,\epsilon_g,\,x_1,\,z_1,\,\omega) \times V_1(x_1,\,z_1,\,x_2,\,z_2,\,\omega) \times P_0^{\mathrm{d}}(x_2,\,z_2,\,x_s,\,\epsilon_s,\,\omega)\mathrm{d}x_1\mathrm{d}z_1\mathrm{d}x_2\mathrm{d}z_2. \tag{A.1}$$

Substituting the bilinear form of Green's function

$$G_0^{\mathrm{d}}(x,\,z,\,x',\,z',\,\omega) = \iint \mathrm{d}k_x\mathrm{d}k_z \frac{\mathrm{e}^{\mathrm{i}k_x(x-x')}\mathrm{e}^{\mathrm{i}k_z(z-z')}}{-k_x^2 - k_z^2 + \frac{\omega^2}{c_0^2}}, \tag{A.2}$$

into equation (A.1), gives

$$D_1'(x_g,\,\epsilon_g,\,x_s,\,\epsilon_s,\,\omega) = \int^{(4)} \iint \mathrm{d}k_x\mathrm{d}k_z \times \frac{\mathrm{e}^{\mathrm{i}k_x(x_g-x_1)}\mathrm{e}^{\mathrm{i}k_z(\epsilon_g-z_1)}}{-k_x^2 - k_z^2 + \frac{\omega^2}{c_0^2}} V_1(x_1,\,z_1,\,x_2,\,z_2,\,\omega) \times P_0^{\mathrm{d}}(x_2,\,z_2,\,x_s,\,\epsilon_s,\,\omega)\mathrm{d}x_1\mathrm{d}z_1\mathrm{d}x_2\mathrm{d}z_2. \tag{A.3}$$

Fourier transforming with respect to $x_g$ and $x_s$ gives

$$\begin{aligned}
D_1'(k_g,\,\epsilon_g,\,k_s,\,\epsilon_s,\,\omega) &= \int^{(4)} \iint \mathrm{d}k_x \mathrm{d}k_z \\
&\times \frac{\mathrm{e}^{\mathrm{i}k_x(x_g-x_1)}\mathrm{e}^{\mathrm{i}k_z(\epsilon_g-z_1)}}{-k_x^2-k_z^2+\frac{\omega^2}{c_0^2}} \int \mathrm{e}^{-\mathrm{i}k_g x_g}\mathrm{d}x_g \\
&\times V_1(x_1,\,z_1,\,x_2,\,z_2,\,\omega) P_0^{\mathrm{d}}(x_2,\,z_2,\,k_s,\,\epsilon_s,\,\omega)\mathrm{d}x_1\mathrm{d}z_1\mathrm{d}x_2\mathrm{d}z_2 \\
&= \int^{(4)} \iint \mathrm{d}k_x \mathrm{d}k_z \frac{\mathrm{e}^{-\mathrm{i}k_x x_1}\mathrm{e}^{\mathrm{i}k_z(\epsilon_g-z_1)}}{-k_x^2-k_z^2+\frac{\omega^2}{c_0^2}} 2\pi\delta(k_x-k_g) \\
&\times V_1(x_1,\,z_1,\,x_2,\,z_2,\,\omega) P_0^{\mathrm{d}}(x_2,\,z_2,\,k_s,\,\epsilon_s,\,\omega)\mathrm{d}x_1\mathrm{d}z_1\mathrm{d}x_2\mathrm{d}z_2 \\
&= 2\pi \int^{(4)} \mathrm{e}^{-\mathrm{i}k_g x_1} \int \mathrm{d}k_z \frac{\mathrm{e}^{\mathrm{i}k_z(\epsilon_g-z_1)}}{-k_z^2 \underbrace{-k_g^2+\frac{\omega^2}{c_0^2}}_{\equiv q_g^2}} V_1(x_1,\,z_1,\,x_2,\,z_2,\,\omega) \\
&\times P_0^{\mathrm{d}}(x_2,\,z_2,\,k_s,\,\epsilon_s,\,\omega)\mathrm{d}x_1\mathrm{d}z_1\mathrm{d}x_2\mathrm{d}z_2 \\
&= 2\pi \int^{(4)} \mathrm{e}^{-\mathrm{i}k_g x_1} \int \mathrm{d}k_z \frac{\mathrm{e}^{\mathrm{i}k_z(\epsilon_g-z_1)}}{-k_z^2+q_g^2} V_1(x_1,\,z_1,\,x_2,\,z_2,\,\omega) \\
&\times P_0^{\mathrm{d}}(x_2,\,z_2,\,k_s,\,\epsilon_s,\,\omega)\mathrm{d}x_1\mathrm{d}z_1\mathrm{d}x_2\mathrm{d}z_2 \\
&= \int^{(4)} \mathrm{e}^{-\mathrm{i}k_g x_1} \frac{\mathrm{e}^{\mathrm{i}k_g|\epsilon_g-z_1|}}{2\mathrm{i}q_g} V_1(x_1,\,z_1,\,x_2,\,z_2,\,\omega) \\
&\times P_0^{\mathrm{d}}(x_2,\,z_2,\,k_s,\,\epsilon_s,\,\omega)\mathrm{d}x_1\mathrm{d}z_1\mathrm{d}x_2\mathrm{d}z_2.
\end{aligned} \tag{A.4}$$

Since we assume $\epsilon_g < z_1$, equation (A.4) becomes

$$\begin{aligned}
D_1'(k_g,\,\epsilon_g,\,k_s,\,\epsilon_s,\,\omega) &= \int^{(4)} \mathrm{e}^{-\mathrm{i}k_g x_1} \frac{\mathrm{e}^{\mathrm{i}k_g(z_1-\epsilon_g)}}{2\mathrm{i}q_g} V_1(x_1,\,z_1,\,x_2,\,z_2,\,\omega) \\
&\times P_0^{\mathrm{d}}(x_2,\,z_2,\,k_s,\,\epsilon_s,\,\omega)\mathrm{d}x_1\mathrm{d}z_1\mathrm{d}x_2\mathrm{d}z_2 \\
&= \frac{\mathrm{e}^{-\mathrm{i}k_g\epsilon_g}}{2\mathrm{i}q_g} \iint V_1(k_g,\,-q_g,\,x_2,\,z_2,\,\omega) P_0^{\mathrm{d}} \\
&\times (x_2,\,z_2,\,k_s,\,\epsilon_s,\,\omega)\mathrm{d}x_2\mathrm{d}z_2.
\end{aligned} \tag{A.5}$$

Similarly, the $n$th-order $D_n'$ is

$$\begin{aligned}
D_n'(k_g,\,\epsilon_g,\,k_s,\,\epsilon_s,\,\omega) &= \frac{\mathrm{e}^{-\mathrm{i}k_g\epsilon_g}}{2\mathrm{i}q_g} \iint V_n'(k_g,\,-q_g,\,x_2,\,z_2,\,\omega) \\
&\times P_0^{\mathrm{d}}(x_2,\,z_2,\,k_s,\,\epsilon_s,\,\omega)\mathrm{d}x_2\mathrm{d}z_2.
\end{aligned} \tag{A.6}$$

Substituting the expression for $P_0^{\mathrm{d}}$ (equation (8)) into equation (A.5), we obtain

$$\begin{aligned}
D_1'(k_g,\,\epsilon_g,\,k_s,\,\epsilon_s,\,\omega) &= \frac{\mathrm{e}^{-\mathrm{i}k_g\epsilon_g}}{2\mathrm{i}q_g} \iint V_1(k_g,\,-q_g,\,x_2,\,z_2,\,\omega)\rho(k_s,\,q_s,\,\omega) \\
&\times \mathrm{e}^{\mathrm{i}k_s x_2}\mathrm{e}^{\mathrm{i}q_s z_2}\frac{\mathrm{e}^{-\mathrm{i}q_s\epsilon_s}}{2\mathrm{i}q_s}\mathrm{d}x_2\mathrm{d}z_2 \\
&= \frac{\mathrm{e}^{-\mathrm{i}k_g\epsilon_g}}{2\mathrm{i}q_g} V_1(k_g,\,-q_g,\,-k_s,\,-q_s,\,\omega)\rho(k_s,\,q_s,\,\omega)\frac{\mathrm{e}^{-\mathrm{i}q_s\epsilon_s}}{2\mathrm{i}q_s}.
\end{aligned} \tag{A.7}$$

The $n$th-order free-surface multiple prediction (equation (3)) is given by

$$\begin{aligned}
D_n'(x_g,\,\epsilon_g,\,x_s,\,\epsilon_s,\,\omega) &= -\int^{(8)} \mathrm{d}x_1\mathrm{d}z_1\mathrm{d}x_2\mathrm{d}z_2 G_0^{\mathrm{d}} \\
&\times (x_g,\,\epsilon_g,\,x_1,\,z_1,\,\omega) V_1(x_1,\,z_1,\,x_2,\,z_2,\,\omega) \\
&\times G_0^{\mathrm{FS}}(x_2,\,z_2,\,x_3,\,z_3,\,\omega) V_{n-1}'(x_3,\,z_3,\,x_4,\,z_4,\,\omega) \\
&\times P_0^{\mathrm{d}}(x_4,\,z_4,\,x_s,\,\epsilon_s,\,\omega)\mathrm{d}x_3\mathrm{d}z_3\mathrm{d}x_4\mathrm{d}z_4.
\end{aligned} \tag{A.8}$$

Substituting the bilinear form of Green's function ($G_0^{\mathrm{d}}$ and $G_0^{\mathrm{FS}}$) into equation (A.8), gives

$$\begin{aligned}
D_n'(x_g,\,\epsilon_g,\,x_s,\,\epsilon_s,\,\omega) &= -\int^{(8)} \mathrm{d}x_1\mathrm{d}z_1\mathrm{d}x_2\mathrm{d}z_2 \\
&\times \iint \mathrm{d}k_{x'}\mathrm{d}k_{z'} \frac{\mathrm{e}^{\mathrm{i}k_{x'}(x_g-x_1)}\mathrm{e}^{\mathrm{i}k_{z'}(\epsilon_g-z_1)}}{-k_{x'}^2-k_{z'}^2+\frac{\omega^2}{c_0^2}} \\
&\times V_1(x_1,\,z_1,\,x_2,\,z_2,\,\omega) \iint \mathrm{d}k\mathrm{d}k_z \\
&\times \frac{\mathrm{e}^{\mathrm{i}k(x_2-x_3)}\mathrm{e}^{\mathrm{i}k_z(z_2+z_3)}}{-k^2-k_z^2+\frac{\omega^2}{c_0^2}} V_{n-1}'(x_3,\,z_3,\,x_4,\,z_4,\,\omega) \\
&\times P_0^{\mathrm{d}}(x_4,\,z_4,\,x_s,\,\epsilon_s,\,\omega)\mathrm{d}x_3\mathrm{d}z_3\mathrm{d}x_4\mathrm{d}z_4,
\end{aligned} \tag{A.9}$$

where $G_0^{\mathrm{d}}$ is form in equation (A.2) and $G_0^{\mathrm{FS}} = \iint \mathrm{d}k_x\mathrm{d}k_z \frac{\mathrm{e}^{\mathrm{i}k_x(x-x')}\mathrm{e}^{\mathrm{i}k_z(z+z')}}{-k_x^2-k_z^2+\frac{\omega^2}{c_0^2}}$. Fourier transforming with respect to $x_g$ and $x_s$ gives

$$\begin{aligned}
D_n'(k_g,\,\epsilon_g,\,k_s,\,\epsilon_s,\,\omega) &= -\int^{(8)} \mathrm{d}x_1\mathrm{d}z_1\mathrm{d}x_2\mathrm{d}z_2 \\
&\times \iint \mathrm{d}k_{x'}\mathrm{d}k_{z'} \frac{\mathrm{e}^{\mathrm{i}k_{x'}(x_g-x_1)}\mathrm{e}^{\mathrm{i}k_{z'}(\epsilon_g-z_1)}}{-k_{x'}^2-k_{z'}^2+\frac{\omega^2}{c_0^2}} \\
&\times \int \mathrm{e}^{-\mathrm{i}k_g x_g}\mathrm{d}x_g V_1(x_1,\,z_1,\,x_2,\,z_2,\,\omega) \\
&\times \iint \mathrm{d}k\mathrm{d}k_z \frac{\mathrm{e}^{\mathrm{i}k(x_2-x_3)}\mathrm{e}^{\mathrm{i}k_z(z_2+z_3)}}{-k^2-k_z^2+\frac{\omega^2}{c_0^2}} \\
&\times V_{n-1}'(x_3,\,z_3,\,x_4,\,z_4,\,\omega) P_0^{\mathrm{d}}(x_4,\,z_4,\,x_s,\,\epsilon_s,\,\omega) \\
&\times \int \mathrm{e}^{\mathrm{i}k_s x_s}\mathrm{d}x_s\mathrm{d}x_3\mathrm{d}z_3\mathrm{d}x_4\mathrm{d}z_4 \\
&= -\int^{(8)} \mathrm{d}x_1\mathrm{d}z_1\mathrm{d}x_2\mathrm{d}z_2 \iint \mathrm{d}k_{x'}\mathrm{d}k_{z'} \\
&\times \frac{\mathrm{e}^{-\mathrm{i}k_{x'}x_1}\mathrm{e}^{\mathrm{i}k_{z'}(\epsilon_g-z_1)}}{-k_{x'}^2-k_{z'}^2+\frac{\omega^2}{c_0^2}} 2\pi\delta(k_{x'}-k_g) \\
&\times V_1(x_1,\,z_1,\,x_2,\,z_2,\,\omega) \iint \mathrm{d}k\mathrm{d}k_z \\
&\times \frac{\mathrm{e}^{\mathrm{i}k(x_2-x_3)}\mathrm{e}^{\mathrm{i}k_z(z_2+z_3)}}{-k^2-k_z^2+\frac{\omega^2}{c_0^2}} V_{n-1}'(x_3,\,z_3,\,x_4,\,z_4,\,\omega) \\
&\times P_0^{\mathrm{d}}(x_4,\,z_4,\,k_s,\,\epsilon_s,\,\omega)\mathrm{d}x_3\mathrm{d}z_3\mathrm{d}x_4\mathrm{d}z_4.
\end{aligned} \tag{A.10}$$

Integrating over $k_{x'}$ gives

$$\begin{aligned}
D_n'(k_g,\,\epsilon_g,\,k_s,\,\epsilon_s,\,\omega) =& -\int^{(8)} \mathrm{d}x_1\mathrm{d}z_1\mathrm{d}x_2\mathrm{d}z_2 2\pi \\
&\times \int \mathrm{d}k_{z'} \frac{\mathrm{e}^{-\mathrm{i}k_g x_1}\mathrm{e}^{\mathrm{i}k_{z'}(\epsilon_g - z_1)}}{\underbrace{-k_{z'}^2}\underbrace{-k_g^2 + \frac{\omega^2}{c_0^2}}_{\equiv q_g^2}} \\
&\times V_1(x_1,\,z_1,\,x_2,\,z_2,\,\omega) \iint \mathrm{d}k\mathrm{d}k_z \\
&\times \frac{\mathrm{e}^{\mathrm{i}k(x_2-x_3)}\mathrm{e}^{\mathrm{i}k_z(z_2+z_3)}}{\underbrace{-k_z^2}\underbrace{-k^2 + \frac{\omega^2}{c_0^2}}_{\equiv q^2}} V_{n-1}'(x_3,\,z_3,\,x_4,\,z_4,\,\omega) \\
&\times P_0^{\mathrm{d}}(x_4,\,z_4,\,k_s,\,\epsilon_s,\,\omega)\mathrm{d}x_3\mathrm{d}z_3\mathrm{d}x_4\mathrm{d}z_4 \\
=& -\int^{(8)} \mathrm{d}x_1\mathrm{d}z_1\mathrm{d}x_2\mathrm{d}z_2\mathrm{e}^{-\mathrm{i}k_g x_1} 2\pi \\
&\times \int \mathrm{d}k_{z'} \frac{\mathrm{e}^{\mathrm{i}k_{z'}(\epsilon_g - z_1)}}{-k_{z'}^2 + q_g^2} V_1(x_1,\,z_1,\,x_2,\,z_2,\,\omega) \\
&\times \iint \mathrm{d}k\mathrm{d}k_z \frac{\mathrm{e}^{\mathrm{i}k(x_2-x_3)}\mathrm{e}^{\mathrm{i}k_z(z_2+z_3)}}{-k_z^2 + q^2} V_{n-1}'(x_3,\,z_3,\,x_4,\,z_4,\,\omega) \\
&\times P_0^{\mathrm{d}}(x_4,\,z_4,\,k_s,\,\epsilon_s,\,\omega)\mathrm{d}x_3\mathrm{d}z_3\mathrm{d}x_4\mathrm{d}z_4 \\
=& -\int^{(8)} \mathrm{d}x_1\mathrm{d}z_1\mathrm{d}x_2\mathrm{d}z_2\mathrm{e}^{-\mathrm{i}k_g x_1} \frac{\mathrm{e}^{\mathrm{i}q_g|\epsilon_g - z_1|}}{2\mathrm{i}q_g} \\
&\times V_1(x_1,\,z_1,\,x_2,\,z_2,\,\omega) \frac{1}{2\pi}\int \mathrm{d}k\mathrm{e}^{\mathrm{i}k(x_2-x_3)} \\
&\times \frac{\mathrm{e}^{\mathrm{i}q|z_2+z_3|}}{2\mathrm{i}q} V_{n-1}'(x_3,\,z_3,\,x_4,\,z_4,\,\omega) \\
&\times P_0^{\mathrm{d}}(x_4,\,z_4,\,k_s,\,\epsilon_s,\,\omega)\mathrm{d}x_3\mathrm{d}z_3\mathrm{d}x_4\mathrm{d}z_4.
\end{aligned} \tag{A.11}$$

Since we assume $\epsilon_g < z_1, z_2 > 0$, and $z_3 > 0$, equation (A.11) becomes

$$\begin{aligned}
D_n'(k_g,\,\epsilon_g,\,k_s,\,\epsilon_s,\,\omega) =& -\int^{(8)} \mathrm{d}x_1\mathrm{d}z_1\mathrm{d}x_2\mathrm{d}z_2\mathrm{e}^{-\mathrm{i}k_g x_1} \\
&\times \frac{\mathrm{e}^{\mathrm{i}q_g(z_1-\epsilon_g)}}{2\mathrm{i}q_g} V_1(x_1,\,z_1,\,x_2,\,z_2,\,\omega) \\
&\times \frac{1}{2\pi}\int \mathrm{d}k\mathrm{e}^{\mathrm{i}k(x_2-x_3)} \frac{\mathrm{e}^{\mathrm{i}q(z_2+z_3)}}{2\mathrm{i}q} V_{n-1}'(x_3,\,z_3,\,x_4,\,z_4,\,\omega) \\
&\times P_0^{\mathrm{d}}(x_4,\,z_4,\,k_s,\,\epsilon_s,\,\omega)\mathrm{d}x_3\mathrm{d}z_3\mathrm{d}x_4\mathrm{d}z_4 \\
=& -\frac{1}{2\pi}\int \mathrm{d}k \frac{\mathrm{e}^{-\mathrm{i}q_g\epsilon_g}}{2\mathrm{i}q_g} \int^{(8)} \mathrm{d}x_1\mathrm{d}z_1\mathrm{d}x_2\mathrm{d}z_2\mathrm{e}^{-\mathrm{i}k_g x_1} \\
&\times \mathrm{e}^{\mathrm{i}q_g z_1} V_1(x_1,\,z_1,\,x_2,\,z_2,\,\omega)\mathrm{e}^{\mathrm{i}kx_2}\mathrm{e}^{\mathrm{i}qz_2}\frac{1}{2\mathrm{i}q} \\
&\times \mathrm{e}^{-\mathrm{i}kx_3}\mathrm{e}^{\mathrm{i}qz_3} V_{n-1}'(x_3,\,z_3,\,x_4,\,z_4,\,\omega) \\
&\times P_0^{\mathrm{d}}(x_4,\,z_4,\,k_s,\,\epsilon_s,\,\omega)\mathrm{d}x_3\mathrm{d}z_3\mathrm{d}x_4\mathrm{d}z_4 \\
=& -\frac{1}{2\pi}\int \mathrm{d}k \frac{\mathrm{e}^{-\mathrm{i}q_g\epsilon_g}}{2\mathrm{i}q_g} V_1(k_g,\,-q_g,\,-k,\,-q,\,\omega)\frac{1}{2\mathrm{i}q} \\
&\times \iint V_{n-1}'(k,\,-q,\,x_4,\,z_4,\,\omega) P_0^{\mathrm{d}}(x_4,\,z_4,\,k_s,\,\epsilon_s,\,\omega)\mathrm{d}x_4\mathrm{d}z_4.
\end{aligned} \tag{A.12}$$

Inserting two identities into equation (A.12) gives

$$\begin{aligned}
D_n'(k_g,\,\epsilon_g,\,k_s,\,\epsilon_s,\,\omega) =& -\frac{1}{2\pi}\int \mathrm{d}k \frac{\mathrm{e}^{-\mathrm{i}q_g\epsilon_g}}{2\mathrm{i}q_g} \\
&\times V_1(k_g,\,-q_g,\,-k,\,-q,\,\omega) \underbrace{\frac{\mathrm{e}^{-\mathrm{i}q\epsilon_s}}{2\mathrm{i}q}\frac{2\mathrm{i}q}{\mathrm{e}^{-\mathrm{i}q\epsilon_s}}}_{1}\frac{1}{2\mathrm{i}q} \\
&\times \underbrace{\frac{2\mathrm{i}q}{\mathrm{e}^{-\mathrm{i}q\epsilon_g}}\frac{\mathrm{e}^{-\mathrm{i}q\epsilon_g}}{2\mathrm{i}q}}_{1} \iint V_{n-1}'(k,\,-q,\,x_4,\,z_4,\,\omega) \\
&\times P_0^{\mathrm{d}}(x_4,\,z_4,\,k_s,\,\epsilon_s,\,\omega)\mathrm{d}x_4\mathrm{d}z_4 \\
=& -\frac{1}{2\pi}\int \mathrm{d}k \underbrace{\frac{\mathrm{e}^{-\mathrm{i}q_g\epsilon_g}}{2\mathrm{i}q_g} V_1(k_g,\,-q_g,\,-k,\,-q,\,\omega)\frac{\mathrm{e}^{-\mathrm{i}q\epsilon_s}}{2\mathrm{i}q}}_{\frac{D_1'(k_g,\epsilon_g,k,\epsilon_s,\omega)}{\rho(k,q,\omega)}} \\
&\times \underbrace{\frac{2\mathrm{i}q}{\mathrm{e}^{-\mathrm{i}q\epsilon_s}}\frac{1}{2\mathrm{i}q}\frac{2\mathrm{i}q}{\mathrm{e}^{-\mathrm{i}q\epsilon_g}}}_{2\mathrm{i}q\mathrm{e}^{\mathrm{i}q(\epsilon_s+\epsilon_g)}} \\
&\times \underbrace{\frac{\mathrm{e}^{-\mathrm{i}q\epsilon_g}}{2\mathrm{i}q} \iint V_{n-1}'(k,\,-q,\,x_4,\,z_4,\,\omega) P_0^{\mathrm{d}}(x_4,\,z_4,\,k_s,\,\epsilon_s,\,\omega)\mathrm{d}}_{D_{n-1}'(k,\epsilon_g,k_s,\epsilon_s,\omega)} \\
=& \frac{1}{\mathrm{i}\pi}\int \frac{\mathrm{d}k}{\rho(k,\,q,\,\omega)} D_1'(k_g,\,\epsilon_g,\,k,\,\epsilon_s,\,\omega) q\mathrm{e}^{\mathrm{i}q(\epsilon_s+\epsilon_g)} \\
&\times D_{n-1}'(k,\,\epsilon_g,\,k_s,\,\epsilon_s,\,\omega) \\
=& \frac{1}{\mathrm{i}\pi}\int \frac{\mathrm{d}k}{\rho(k,\,q,\,\omega)} D_1'(k_g,\,k,\,\omega) q\mathrm{e}^{\mathrm{i}q(\epsilon_s+\epsilon_g)} D_{n-1}'(k,\,k_s,\,\omega).
\end{aligned} \tag{A.13}$$

In the above derivation, equations (A.6) and (A.7) are applied. In the final step, we ignore the constant variables $\epsilon_s$ and $\epsilon_g$ in the data $D_1'$ and $D_{n-1}'$. Equation (A.13) is the extended ISS FSME algorithm.

## Appendix B. Derivation of equation (8)

The projection of a general source signature $\rho(k,\,q,\,\omega)$ is derived from the direct reference wavefield $P_0^{\mathrm{d}}$. We assume for simplicity that the distribution of the general source is the same for each experiment, which means that the source distribution does not depend on the effective source position $r_s$. Thus, $P_0^{\mathrm{d}}$ in a 2D case can be presented as equation (7)

$$\begin{aligned}
P_0^{\mathrm{d}}(x,\,z,\,x_s,\,z_s,\,\omega) =& \iint \mathrm{d}x'\mathrm{d}z'\rho(x',\,z',\,\omega) \\
&\times G_0^{\mathrm{d}}(x,\,z,\,x'+x_s,\,z'+z_s,\,\omega),
\end{aligned} \tag{B.1}$$

where $(x',\,z')$ is the source distribution with respect to the effective source position $(x_s,\,z_s)$. Using the bilinear form of Green's function,

$$\begin{aligned}
G_0^{\mathrm{d}}(x,\,z,\,x'+x_s,\,z'+z_s,\,\omega) =& \iint \mathrm{d}k_x\mathrm{d}k_z \\
&\times \frac{\mathrm{e}^{\mathrm{i}k_x(x-x'-x_s)}\mathrm{e}^{\mathrm{i}k_z(z-z'-z_s)}}{-k_x^2 - k_z^2 + \frac{\omega^2}{c_0^2}},
\end{aligned} \tag{B.2}$$

equation (B.1) becomes

$$P_0^{\mathrm{d}}(x, z, x_s, z_s, \omega) = \iint \mathrm{d}x'\mathrm{d}z'\rho(x', z', \omega) \times \iint \mathrm{d}k_x\mathrm{d}k_z \frac{\mathrm{e}^{\mathrm{i}k_x(x-x'-x_s)}\mathrm{e}^{\mathrm{i}k_z(z-z'-z_s)}}{-k_x^2 - k_z^2 + \frac{\omega^2}{c_0^2}}. \quad \text{(B.3)}$$

We apply the following convention for Fourier transforms

$$P(k) = \int p(x)\mathrm{e}^{-\mathrm{i}kx}\mathrm{d}x,$$

$$p(x) = 2\pi \int P(k)\mathrm{e}^{\mathrm{i}kx}\mathrm{d}k$$

and take Fourier transform with respect to $x$ on both sides of equation (B.3)

$$\begin{aligned} P_0^{\mathrm{d}}(k, z, x_s, z_s, \omega) &= \iint \mathrm{d}x'\mathrm{d}z'\rho(x', z', \omega) \iint \mathrm{d}k_x\mathrm{d}k_z \\ &\times \frac{\mathrm{e}^{\mathrm{i}k_x(x-x'-x_s)}\mathrm{e}^{\mathrm{i}k_z(z-z'-z_s)}}{-k_x^2 - k_z^2 + \frac{\omega^2}{c_0^2}} \int \mathrm{e}^{-\mathrm{i}kx}\mathrm{d}x \\ &= \iint \mathrm{d}x'\mathrm{d}z'\rho(x', z', \omega) \\ &\times \iint \mathrm{d}k_x\mathrm{d}k_z \frac{\mathrm{e}^{\mathrm{i}k_x(-x'-z_s)}\mathrm{e}^{\mathrm{i}k_z(z-z'-z_s)}}{-k_x^2 - k_z^2 + \frac{\omega^2}{c_0^2}} 2\pi\delta(k_x - k) \\ &= \iint \mathrm{d}x'\mathrm{d}z'\rho(x', z', \omega) 2\pi \int \mathrm{d}k_z \frac{\mathrm{e}^{\mathrm{i}k(-x'-x_s)}\mathrm{e}^{\mathrm{i}k_z(z-z'-z_s)}}{-k_z^2 \underbrace{-k^2 + \frac{\omega^2}{c_0^2}}_{\equiv q^2}} \\ &= \iint \mathrm{d}x'\mathrm{d}z'\rho(x', z', \omega)\mathrm{e}^{\mathrm{i}k(-x'-x_s)} 2\pi \int \mathrm{d}k_z \frac{\mathrm{e}^{\mathrm{i}k_z(z-z'-z_s)}}{-k_z^2 + q^2} \\ &= \iint \mathrm{d}x'\mathrm{d}z'\rho(x', z', \omega)\mathrm{e}^{\mathrm{i}k(-x'-x_s)} \frac{\mathrm{e}^{\mathrm{i}q|z-z'-z_s|}}{2\mathrm{i}q} \\ &= \iint \mathrm{d}x'\mathrm{d}z'\rho(x', z', \omega)\mathrm{e}^{\mathrm{i}k(-x'-x_s)} \frac{\mathrm{e}^{\mathrm{i}q(z-z'-z_s)}}{2\mathrm{i}q} \\ &= \rho(k, q, \omega)\mathrm{e}^{-\mathrm{i}kx_s}\mathrm{e}^{-\mathrm{i}qz_s} \frac{\mathrm{e}^{\mathrm{i}qz}}{2\mathrm{i}q}. \end{aligned} \quad \text{(B.4)}$$

Here, $z > (z' + z_s)$ is used, because the prediction point is deeper than the source distribution.

## References


Amundsen L 1993 Estimation of source array signature *Geophysics* **58** 1865–9

Berkhout A J and Verschuur D J 1999 Removal of internal multiples *69th Annual Int. Meeting, SEG, Expanded Abstracts* pp 1334–7

Carvalho P M 1992 Free-surface multiple reflection elimination method based on nonlinear inversion of seismic data *PhD Thesis* Universidade Federal da Bahia

Dragoset W H, Moore I, Yu M and Zhao W 2008 Removal of internal multiples *78th Annual Int. Meeting, SEG, Expanded Abstracts* pp 2426–30

Ikelle L T, Roberts G and Weglein A B 1997 Source signature estimation based on the removal of the first-order multiples *Geophysics* **62** 1904–20

Loveridge M M, Parkes G E, Hatton L and Worthington M H 1984 Effects of marine source array directivity on seismic data and source signature deconvolution *First Break* **2** 16–22

Mayhan J D and Weglein A B 2013 First application of Green's theorem-derived source and receiver deghosting on deep-water Gulf of Mexico synthetic (SEAM) and field data *Geophysics* **78** WA77–89

Mayhan J D, Weglein A B and Terenghi P 2012 First application of Green's theorem derived source and receiver deghosting on deep water Gulf of Mexico synthetic (SEAM) and field data *82nd Annual Int. Meeting, SEG, Expanded Abstracts* pp 1–5

Mayhan J, Terenghi P, Weglein A B and Chemingui N 2011 Green's theorem derived methods for preprocessing seismic data when the pressure $P$ and its normal derivative are measured *81st Annual Int. Meeting, SEG, Expanded Abstracts* pp 2722–6

Osen A, Bruce G S and Lasse A 1998 Wavelet estimation from marine pressure measurements *Geophysics* **63** 2108–19

Tang L, Mayhan J D, Yang J and Weglein A B 2013 Using Green's theorem to satisfy data requirements of inverse scattering series multiple removal methods *83rd Int. Annual Meeting, SEG, Expanded Abstracts* pp 4392–6

Verschuur D J, Berkhout A J and Wapenaar C P A 1990 Surface-related mutiple elimination in the presence of near-surface anomolies *Geophysics* **57** 1166

Weglein A B, Araújo F V, Carvalho P M, Stolt R H, Matson K H, Coates R T, Corrigan D, Foster D J, Shaw S A and Zhang H 2003 Inverse scattering series and seismic exploration *Inverse Problems* **19** R27–83

Weglein A B, Foster D J, Matson K H, Shaw S A, Carvalho P M and Corrigan D 2002 Predicting the correct spatial location of reflectors without knowing or determining the precise medium and wave velocity: initial concept, algorithm and analytic and numerical example *J. Seismic Explor.* **10** 367–82

Weglein A B, Gasparotto F A, Carvalho P M and Stolt R H 1997 An inverse-scattering series method for attenuating multiples in seismic reflection data *Geophysics* **62** 1975–89

Weglein A B and Secrest B G 1990 Wavelet estimation for a multidimensional acoustic earth model *Geophysics* **55** 902–13

Wu J and Weglein A B 2014 Elastic Green's theorem preprocessing for on-shore internal multiple attenuation: theory and initial synthetic data tests *84th Annual Int. Meeting, SEG, Expanded Abstracts* pp 4299–304

Yang J 2014 Extending the inverse scattering series free-surface multiple elimination and internal multiple attenuation algorithms by incorporating the source wavelet and radiation pattern: examining and evaluating the benefit and added-value *PhD Thesis* University of Houston

Yang J and Weglein A B 2015 Accommodating the source wavelet and radiation pattern in the internal multiple attenuation algorithm: theory and initial example that demonstrates impact *85th Int. Annual Meeting, SEG, Expanded Abstracts* pp 4396–401

Zhang J 2007 Wave theory based data preparation for inverse scattering multiple removal, depth imaging and parameter estimation: analysis and numerical tests of Green's theorem deghosting theory *PhD Thesis* University of Houston

Zhang J and Weglein A B 2005 Extinction theorem deghosting method using towed streamer pressure data: analysis of the receiver array effect on deghosting and subsequent free surface multiple removal *75th Int. Annual Meeting, SEG, Expanded Abstracts* pp 2095–98

Zhang J and Weglein A B 2006 Application of extinction theorem deghosting method on ocean bottom data *76th Int. Annual Meeting, SEG, Expanded Abstracts* pp 2674–8